JOURNAL OF VIROLOGY, Nov. 2010, p. 11590–11598 Vol. 84, No. 21
0022-538X/10/$12.00 doi:10.1128/JVI.00587-10

Hepatitis C Virus Egress and Release Depend on Endosomal Trafficking of Core Protein▽

Chao-Kuen Lai,[1] King-Song Jeng,[1] Keigo Machida,[2] and Michael M. C. Lai[1,2,3]*

Institute of Molecular Biology, Academia Sinica, Taipei 115, Taiwan[1]; Department of Molecular Microbiology and Immunology, University of Southern California, Keck School of Medicine, 2001 Zonal Avenue, Los Angeles, California 90033[2]; and National Cheng Kung University, Tainan 701, Taiwan[3]

Received 17 March 2010/Accepted 13 August 2010

Hepatitis C virus (HCV) assembly is known to occur in juxtaposition to lipid droplets, but the mechanisms of nascent virion transport and release remain poorly understood. Here we demonstrate that HCV core protein targets to early and late endosomes but not to mitochondria or peroxisomes. Further, by employing inhibitors of early and late endosome motility in HCV-infected cells, we demonstrate that the movement of core protein to the early and late endosomes and virus production require an endosome-based secretory pathway. We also observed that this way is independent of that of the internalization of endocytosed virus particles during virus entry.

Hepatitis C virus (HCV) is a major causative agent of chronic hepatitis, liver cirrhosis, and hepatocellular carcinoma. HCV usually infects host cells via receptor-mediated endocytosis (6, 21), followed by the release of genomic RNA after uncoating of the nucleocapsid in the endosome. HCV core protein constitutes the viral nucleocapsid and may possess multiple functions. Intracellular HCV core protein is localized mainly in lipid droplets (LDs) (23, 29). Recent studies have indicated that core protein promotes the accumulation of LDs to facilitate virus assembly (1, 10) and recruits viral replication complexes to LD-associated membranes, where virus assembly takes place (23). However, the precise mechanisms of HCV assembly, budding, and release remain largely unclear. Most recently, HCV virion release has been shown to require the functional endosomal sorting complex required for transport III (ESCRT-III) and Vps4 (an AAA ATPase) (13), which are required for the biogenesis of the multivesicular body (MVB), a late endosomal compartment (12). Late endosomes have been implicated in the budding of several other viruses, including retroviruses (8, 17, 24, 25, 27), rhabdoviruses (14), filoviruses (18, 20), arenaviruses (26, 32), and hepatitis B virus (35). However, little is known about the roles of late endosomes in the HCV life cycle.

Since LDs are associated with the endoplasmic reticulum membrane, endosomes, peroxisomes, and mitochondria (16, 37), we investigated what subcellular compartments may be involved in HCV assembly and release. We first compared the intracellular distribution of HCV core protein with that of early endosome markers Rab5a and early endosome antigen 1 (EEA1), as well as the late endosome marker CD63 in the HCV Jc1-infected Huh7.5 cells at day 10 postinfection (p.i.). In immunofluorescence studies, we demonstrated that the core protein partially colocalized with Rab5a (Fig. 1A, left panel) or EEA1 (Fig. 1A, right panel). This finding was confirmed by the expression of enhanced green fluorescent protein (EGFP)-tagged Rab5a (Fig. 1A, middle panel). Similarly, core protein also showed partial colocalization with CD63 (Fig. 1B). In particular, core protein showed numerous vesicle-like structures of homogeneous size that partially colocalized with CD63 at the cell periphery (Fig. 1B, right panel inset and drawing). This result contrasts with that of Ai et al. (2), who observed, by confocal microscopy, that core protein did not interact with markers of early and late endosomes. Ai et al. did find, however, that multimeric core complexes cofractionated with ER/late endosomal membranes in HCV-infected cells.

To demonstrate the specificity of the association of core protein with endosomes, we transfected HCV-infected cells (at day 10 p.i.) with pEYFP, pEYFP-mito, and pEYFP-peroxi (Clontech) (Fig. 1C), which label the cytoplasm/nucleus, mitochondria, and peroxisomes, respectively. The results showed that HCV core protein did not colocalize with mitochondria or peroxisomes. Taken together, these results indicate that core protein is partially associated with early and late endosomes.

To investigate the functional involvement of the endosomes in HCV release, we employed HCV-infected cells (at day 10 p.i.). In our observation, at day 10 p.i., not all the cells were infected with HCV, as revealed by immunofluorescence staining against core protein (data not shown), suggesting that these cells are a mixture of infected and noninfected cells. We examined the effects of inhibitors of endosome movement, including 10 μM nocodazole (which induces microtubule depolymerization), 100 nM wortmannin (which inhibits early endosomes), 20 nM Baf-A1 (which blocks early endosomes from fusing with late endosomes) (Sigma), and 10 μg/ml U18666A (which arrests late endosome movement) (Biomol), on the release of HCV in the HCV-infected cells. We first determined the possible cytotoxicity of these drugs. We found that within 20 h of the drug application, no significant effect on cell viability, as revealed by 3-(4,5-dimethylthiazol-2-yl)-5-(3-carboxymethoxyphenyl)-2-(4-sulfophenyl)-2H-tetrazolium salt (MTS) assay, was observed (Fig. 2C). We therefore treated the

* Corresponding author. Mailing address: Institute of Molecular Biology, Academia Sinica, Taipei 115, Taiwan. Phone: 886-2-27892365. Fax: 886-2-27826085. E-mail: michlai@gate.sinica.edu.tw.

▽ Published ahead of print on 25 August 2010.

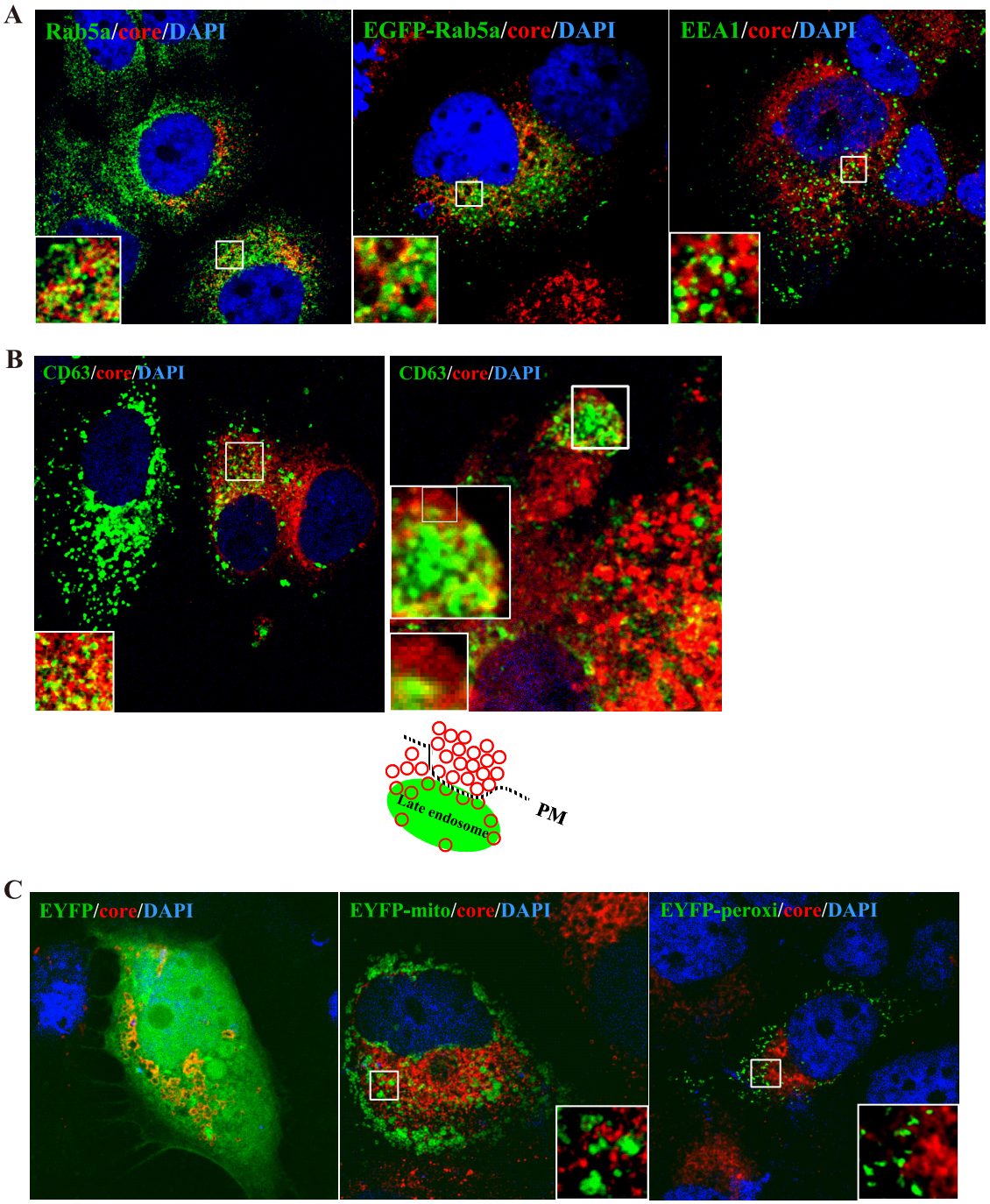

FIG. 1. HCV core protein colocalized with early and late endosomes but not mitochondria and peroxisomes. HCV-infected cells were costained with anti-core protein (red) and anti-Rab5a (A, left panel), -EEA1 (A, right panel), or -CD63 antibodies (green) (B) or transfected with plasmids expressing enhanced green fluorescent protein (EGFP)-Rab5a (A, middle panel), enhanced yellow fluorescent protein (EYFP) (C, left panel), EYFP-mitochondria (C, middle panel), or EYFP-peroxisome (C, right panel). Cellular DNA was labeled with DAPI (4′,6-diamidine-2-phenylindole) (blue). Images shown were collected sequentially with a confocal laser scanning microscope and merged to demonstrate colocalization (yellow merge fluorescence). Enlarged views of parts of every image are shown (insets). The cartoon in panel B illustrates the core protein-containing vesicle-like structures (depicted as red circles), which partially colocalized with CD63 at the cell periphery in HCV-infected cells. PM, plasma membrane.

cells with the various drugs for 20 h. This protocol focuses only on virus release, not on virus entry, as the reinfection of Huh7.5 cells could not account for the effects on virus release, as one round of HCV replication requires about 24 h (11).

After treatments for 20 h, the cells and their culture supernatants were collected. Intracellular RNA was isolated from cell lysates using a High Pure RNA isolation kit (Roche), and viral RNA was isolated from cell culture supernatants using a

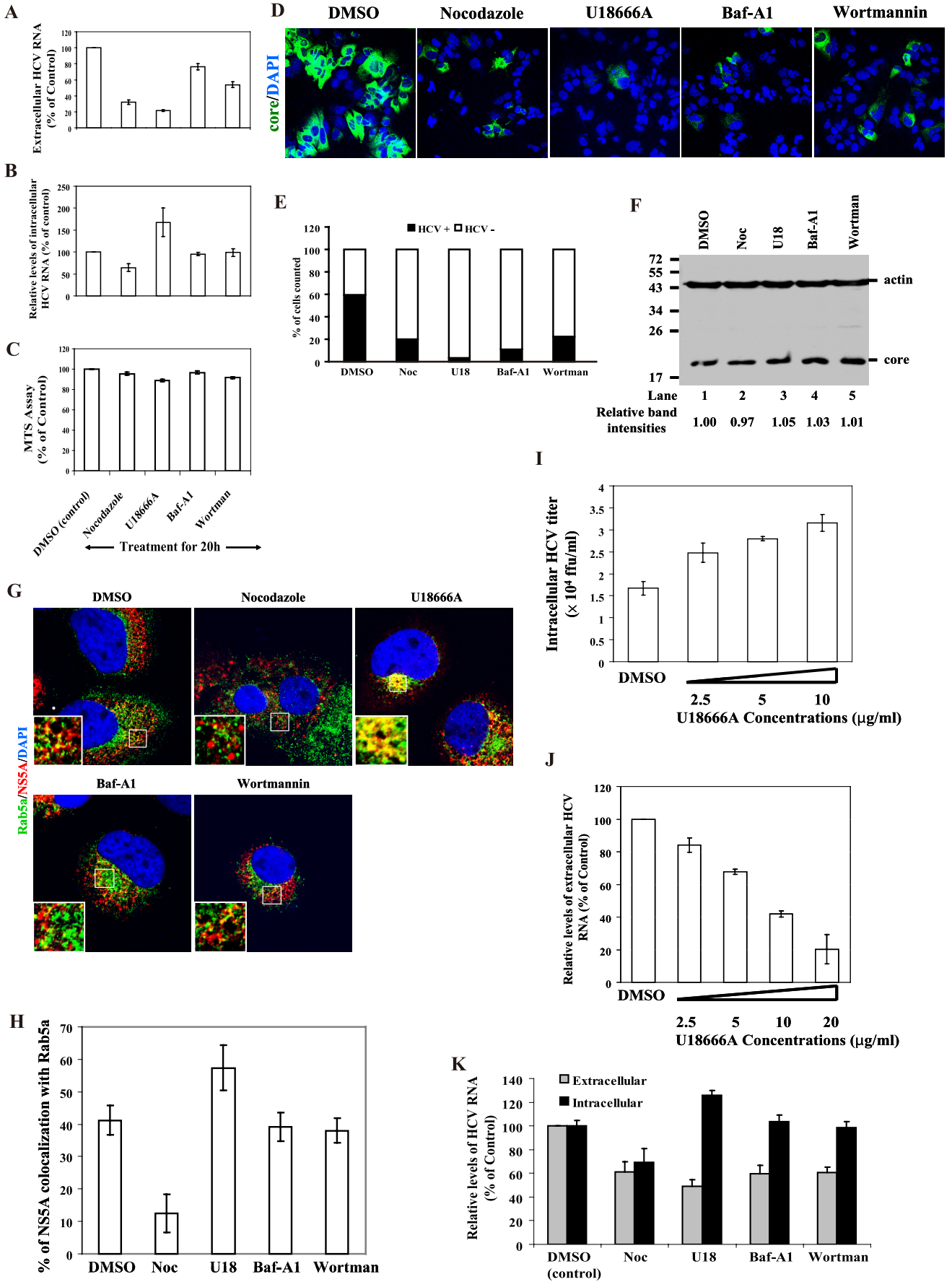
A
Extracellular HCV RNA (% of Control)
B
Relative levels of intracellular HCV RNA (% of control)
C
MTS Assay (% of Control)
DMSO (control)
Nocodazole
U18666A
Baf-A1
Wortman
Treatment for 20h
D
DMSO
Nocodazole
U18666A
Baf-A1
Wortmannin
core/DAPI
E
HCV + HCV -
% of cells counted
DMSO
Noc
U18
Baf-A1
Wortman
F
DMSO
Noc
U18
Baf-A1
Wortman
72
55
43
34
26
17
actin
core
Lane 1 2 3 4 5
Relative band intensities 1.00 0.97 1.05 1.03 1.01
G
DMSO
Nocodazole
U18666A
Baf-A1
Wortmannin
Rab5a/NS5A/DAPI
H
% of NS5A colocalization with Rab5a
DMSO
Noc
U18
Baf-A1
Wortman
I
Intracellular HCV titer (× 10⁴ ffu/ml)
DMSO
2.5
5
10
U18666A Concentrations (μg/ml)
J
Relative levels of extracellular HCV RNA (% of Control)
DMSO
2.5
5
10
20
U18666A Concentrations (μg/ml)
K
Extracellular
Intracellular
Relative levels of HCV RNA (% of Control)
DMSO (control)
Noc
U18
Baf-A1
Wortman

QIAamp viral RNA kit (Qiagen). Equivalent RNA volumes were subsequently analyzed on a LightCycler 1.5 real-time PCR system (Roche) for quantitative PCR (qPCR), with a primer-probe set specific for the 5′ untranslated region (UTR) sequence of HCV Jc1 and a second set specific for the glyceraldehyde-3-phosphate dehydrogenase (GAPDH) gene to quantitate the RNA amount. To calculate the percentage of HCV RNA remaining after the inhibitor treatments, the mean HCV RNA levels from triplicate wells of each sample type were standardized to the mean GAPDH RNA level in the dimethyl sulfoxide (DMSO) control wells. The relative levels of HCV RNA (percentage of control) were then analyzed with LightCycler software (version 3.53) and calculated using the relative quantification method as described in Roche Applied Science, Relative Quantification, Technical Note no. LC 13/2001 (http://www.gene-quantification.de/roche-rel-quant.pdf).

As indicated in Fig. 2A, the extracellular HCV RNA levels were reduced to 32.1%, 21.7%, 76.2%, and 53.8% of the DMSO control after treatments with nocodazole, U18666A, Baf-A1, and wortmannin, respectively. We further determined the intracellular levels of HCV RNA to test whether these drugs have an effect on HCV RNA replication. Intracellular HCV RNA was reduced to 64% by nocodazole treatment (Fig. 2B), confirming previous reports that microtubules are required for HCV RNA synthesis (9, 28). Treatments with Baf-A1 and wortmannin, however, did not affect HCV RNA replication. Interestingly, the intracellular HCV RNA level was increased to 167% by U18666A treatment (Fig. 2B), suggesting that U18666A blocks HCV particle release (Fig. 2A), thereby causing accumulation of HCV RNA in the late endosomes. We further determined the extracellular viral infectivity after treatments with these drugs by using the culture supernatant to infect naïve Huh7.5 cells. The infectivity was checked by counting core protein-expressing cells. Raw acquired 8-bit images (Fig. 2D) were converted to 16-bit and analyzed with the Multi Wavelength Cell Scoring application module in Metamorph (Molecular Device). All of these treatments significantly inhibited the production of infectious HCV particles, as shown by the reduced infectivity in the supernatant of the infected cells (Fig. 2D and E). Determination of the amounts of core protein in the lysates showed that the levels of core protein in cells were not significantly affected by the various drug treatments (Fig. 2F). Taken together, these results suggest that the inhibitors of endosome movement, including U18666A, Baf-A1, and wortmannin, reduced the secretion of HCV particles but not the HCV RNA replication. On the other hand, nocodazole-induced microtubule depolymerization reduced both HCV RNA synthesis (Fig. 2B) (9, 28) and virus release (Fig. 2A and E). Since nocodazole also blocks the movement of endosomes between pericentriolar regions and the cell periphery (3, 7), it therefore should perturb particle release. Our present results show that nocodazole had a greater effect on the reduction in extracellular HCV RNA levels (to 32%) than intracellular HCV RNA levels (to 64%) (Fig. 2A and B), and this effect may be due to blocking of endosome movement and reduced HCV RNA replication. These results can be explained on the premise that nocodazole treatments may affect both HCV RNA replication and virus release; it led us to conclude that microtubules may simultaneously play a key role in both HCV RNA replication and virus egress. Thus, both microtubules and the movement of endosomes are required for HCV particle egress.

Earlier reports indicated that Rab5, an early endosomal protein, interacts with NS4B (31) and is required for HCV RNA replication. This effect was demonstrated in Rab5 small interfering RNA (siRNA)-transfected replicon cells (5, 31). However, in our current studies (Fig. 2B) treatments with endosome inhibitors did not reduce the levels of intracellular HCV RNA. In order to investigate the discrepancy between our results and the earlier studies, we examined the effects of endosome inhibitors on the colocalization of NS5A with Rab5a in the HCV-infected cells (at day 10 p.i.) by calculating the percentage of colocalization in the cells. Colocalization scatter diagrams were generated using the colocalization function of the Zeiss LSM Zen software. The weighted colocalization coefficient, defined as the sum of intensities of colocalizing pixels for NS5A with Rab5a in comparison to the overall sum of pixel intensities (above threshold) for NS5A, was determined. Under control conditions (DMSO), NS5A was colocalized with Rab5a throughout the cytoplasm and perinuclear region (Fig. 2G, upper left panel). The proportion of NS5A that colocalized with Rab5a was 41% (Fig. 2H). After treatment with

FIG. 2. HCV virion release requires endosome motility. HCV-infected cells (at day 10 p.i.) were treated with DMSO, nocodazole (10 μM), U18666A (10 μg/ml), Baf-A1 (20 nM), or wortmannin (100 nM) for 20 h, and then the levels of extracellular (A) and intracellular (B) HCV RNA and HCV core proteins (F) in cells were analyzed by RT-qPCR and Western blotting, respectively. Results of Western blotting were quantified by PhosphorImager counting. (C) Analysis of cellular proliferation and survival by MTS assay. (D) Assay of extracellular viral infectivity. The culture supernatants from the cells treated with the various drugs as indicated were used to infect naïve Huh7.5 cells. The cells were stained with anti-core protein antibody (green) and DAPI (blue). The images were analyzed by using Metamorph, and the proportion of cells (of 5,000 counted) expressing core protein was counted (E). Results are presented as percentages and are averages and standard deviations from results of triplicate experiments. (G) In parallel, the HCV-infected cells were costained with anti-Rab5a (green) and -NS5A (red) antibodies. Cellular DNA was labeled with DAPI (blue). Enlarged views of parts of every image are shown (insets). (H) Colocalization efficiency between NS5A and early endosomes was analyzed by using Zeiss LSM Zen software. Error bars represent standard deviations of the mean result from 20 cells of two experiments. (I) Assay of intracellular HCV titers. Intracellular HCV particles were prepared from the HCV-infected cells (at day 10 p.i.) treated with U18666A at concentrations varying from 2.5 to 10 μg/ml for 20 h. The titers of intracellular HCV particles were determined by immunofluorescence staining for core-positive cell foci and are reported in focus-forming units (FFU)/ml. (J) HCV-infected cells (at day 10 p.i.) were treated with U18666A at concentrations varying from 2.5 to 20 μg/ml for 8 h, and then the levels of extracellular HCV RNA were analyzed by RT-qPCR. (K) Effects of nocodazole (10 μM), U18666A (10 μg/ml), Baf-A1 (20 nM), or wortmannin (100 nM) on HCV production in single-cycle HCV growth assays. Huh7.5 cells were infected with HCV at an MOI of 1 and then incubated with DMEM containing the various drugs. At 24 h p.i., the cells and their culture supernatants were collected and used to determine the levels of intracellular and extracellular HCV RNA, which were converted to percentages of the control levels (DMSO) as 100%. Noc, nocodazole; U18, U18666A; Baf-A1, Bafilomycin A1; Wortman, wortmannin.

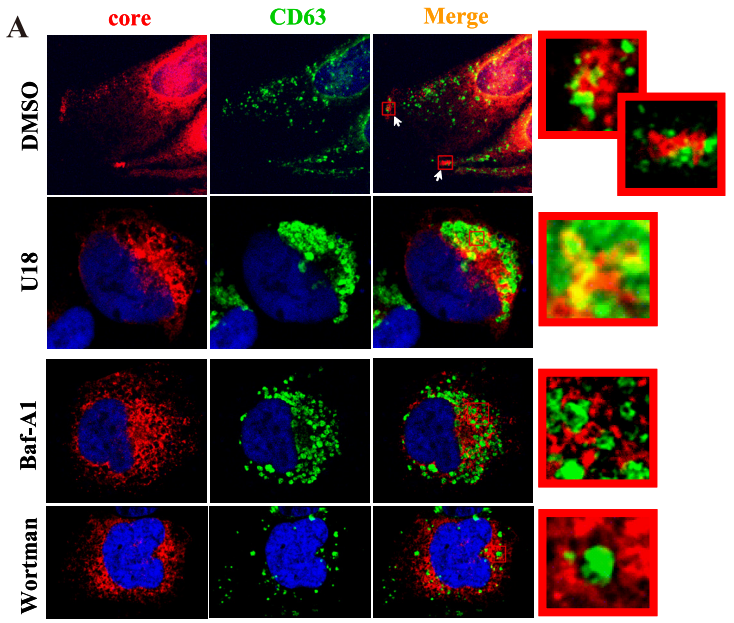
A
core
CD63
Merge
DMSO
U18
Baf-A1
Wortman

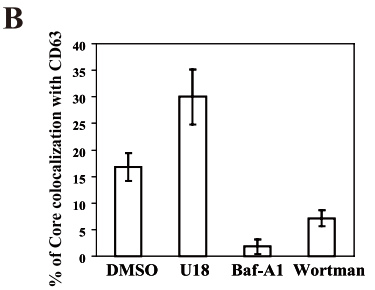
B
% of Core colocalization with CD63
40
35
30
25
20
15
10
5
0
DMSO
U18
Baf-A1
Wortman

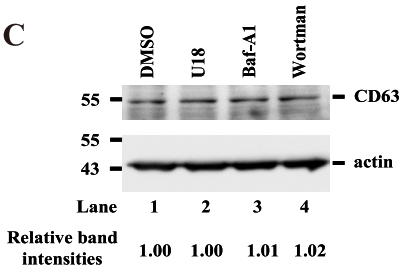
C
DMSO
U18
Baf-A1
Wortman
55
CD63
55
43
actin
Lane 1 2 3 4
Relative band intensities
1.00 1.00 1.01 1.02

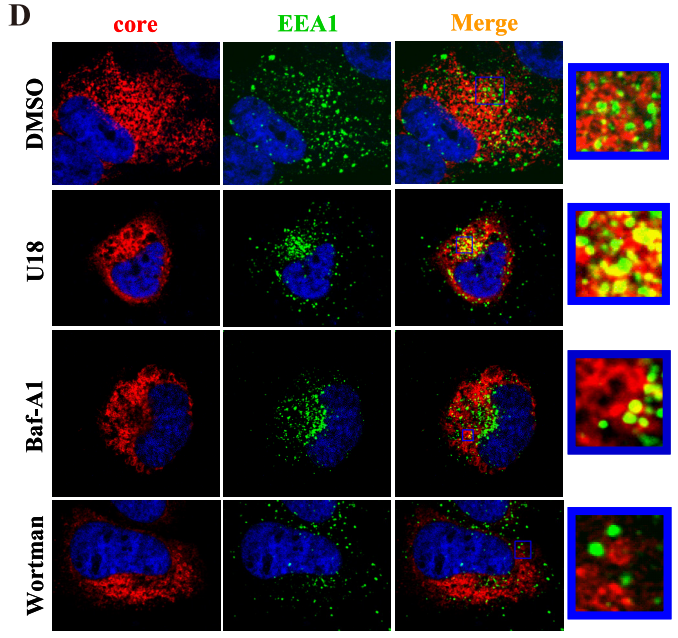
D
core
EEA1
Merge
DMSO
U18
Baf-A1
Wortman

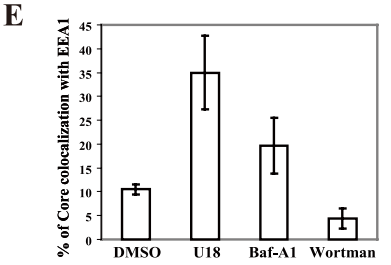
E
% of Core colocalization with EEA1
45
40
35
30
25
20
15
10
5
0
DMSO
U18
Baf-A1
Wortman

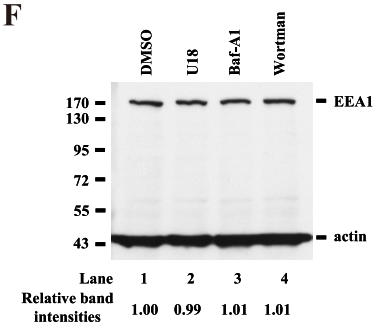
F
DMSO
U18
Baf-A1
Wortman
170
130
95
72
55
43
EEA1
actin
Lane 1 2 3 4
Relative band intensities
1.00 0.99 1.01 1.01

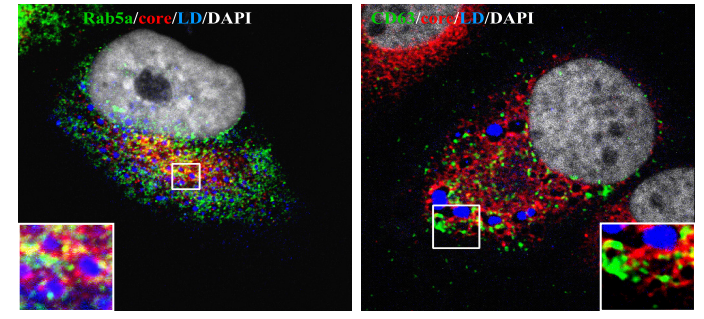
G
Rab5a/core/LD/DAPI
CD63/core/LD/DAPI

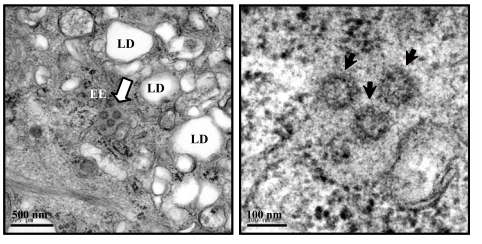
H
LD
EE
LD
LD
500 nm
100 nm

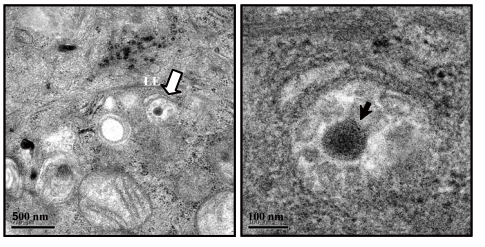
I
LE
500 nm
100 nm

U18666A, the dispersed Rab5a compartments were found only in the perinuclear region (Fig. 2G, upper right panel). Importantly, the colocalization of NS5A with Rab5a was increased to 57% by U18666A treatment. Treatments with Baf-A1 and wortmannin, however, had no significant effect. In contrast, nocodazole treatment reduced the colocalization of NS5A with Rab5a to 12% (Fig. 2G and 2H). Previous studies have reported that the expression levels of Rab5 and its colocalization with HCV NS4B (or NS5A) play a functional role in HCV RNA replication (31). In addition, Rab5 remained in an early endosome fraction and the expression levels of Rab5 showed no significant difference between wortmannin (100 nM)-treated or untreated cells (22). More importantly, the total levels of early endosome proteins, including EEA1 (Fig. 3F) and Rab5a (data not shown), are not altered by the endosome inhibitors. The colocalization efficiency of NS5A with Rab5a was not reduced by U18666A, Baf-A1, or wortmannin treatments, suggesting that these drugs cannot decrease HCV RNA replication. This finding is consistent with the previous results (Fig. 2B). These findings suggest that the observed discrepancy between our results in Fig. 2B and those of the other studies (5, 31) is most likely due to differences in the expression levels of Rab5a.

To further confirm that U18666A suppresses HCV release and/or virus assembly, we determined the titer of the accumulated infectious virus particles inside the cells. The HCV-infected cells (at day 10 p.i.) were treated with U18666A at various concentrations between 2.5 and 10 μg/ml for 20 h, and then intracellular HCV particles were isolated from the cells by repeated freezing and thawing (15). The infectivity was assayed on naïve Huh7.5 cells. The results showed that the titers of infectious intracellular HCV particles were increased in a dose-dependent manner by the U18666A treatments (Fig. 2I). These data, combined with our previous results (Fig. 2A, B, D, and E), indicate that U18666A blocks HCV particle release. Further, we determined the 50% effective dose (ED_{50}) and 50% cytotoxic concentration (CC_{50}), which are defined as the concentration of U18666A that reduced the levels of extracellular HCV RNA by 50% and the concentration of U18666A that produced 50% cytotoxicity in an MTS assay, respectively. We observed that the HCV-infected cells (at day 10 p.i.) treated with U18666A at concentrations varying from 2.5 to 20 μg/ml for 8 h showed a dose-dependent reduction in extracellular HCV RNA levels (Fig. 2J). The ED_{50} and CC_{50} were calculated by polynomial regression analysis. An ED_{50} of 8.18 μg/ml (19.2 μM) and a CC_{50} of 40.26 μg/ml (94.9 μM) were observed for U18666A for the reduction of extracellular HCV RNA and the cytotoxicity of HCV-infected cells, respectively. These results indicate that U18666A acts as a specific inhibitor of HCV release.

In our previous results in Fig. 2A and D, we used a multiple-cycle virus growth assay, which could not discriminate the role of endosome movement in infection from that in virus assembly or egress. We therefore used a single-cycle HCV growth assay to further confirm that these endosome inhibitors could suppress HCV release. Previous studies have suggested that one round of HCV replication requires about 24 h (11). Therefore, Huh7.5 cells were infected with HCV JC1 at a multiplicity of infection (MOI) of 1 for 3 h. The HCV-infected cells were washed with phosphate-buffered saline (PBS) and then incubated with Dulbecco modified Eagle medium (DMEM) containing 10% fetal bovine serum (FBS) and nocodazole (10 μM), U18666A (10 μg/ml), Baf-A1 (20 nM), or wortmannin (100 nM). Therefore, the experiment will focus on virus egress and RNA replication instead of virus entry because the cells were first inoculated with HCV and then treated with the various drugs. At 24 h p.i., the cells and their culture supernatants were collected. Intracellular RNA and viral RNA were isolated from cell lysates and cell culture supernatants, respectively. The percentage of HCV RNA remaining after the inhibitor treatments was determined in the same way as for Fig. 2A and B. As indicated in Fig. 2K, the levels of extracellular HCV RNA (or viral particles) were reduced to 61%, 48.8%, 59.7%, and 60.4% after treatments with nocodazole, U18666A, Baf-A1, and wortmannin, respectively, compared to the control DMSO treatment. We further determined the intracellular levels of HCV RNA to test whether these drugs have an effect on HCV RNA replication. Intracellular HCV RNA was reduced to 69% by nocodazole treatment (Fig. 2K), but not by U18666A, Baf-A1, and wortmannin. Overall, these results of single-cycle HCV growth assay are similar to those of multiple-cycle virus growth assay (Fig. 2A and B), again suggesting that the endosome movement inhibitors reduced the secretion of HCV particles.

To further understand the roles of the early and late endosomes in the HCV life cycle, we next examined the effects of endosome inhibitors on the colocalization of core protein with CD63 or EEA1 in the HCV-infected cells (at day 10 p.i.) by calculating the percentage of their colocalization in the cells. The percentage of colocalization of core protein with CD63 or EEA1 was determined in the same way as for Fig. 2H. Under control conditions (DMSO), core protein was colocalized with CD63 throughout the cytoplasm, perinuclear region, and cell periphery (Fig. 3A, top row). The proportion of core protein

FIG. 3. HCV particles formed are transported from early to late endosomes. HCV-infected cells (at day 10 p.i.) were treated with the various drugs and 14 h later labeled with antibodies specific for core protein (red) and CD63 (green) (A) or EEA1 (green) (D). At the right is an enlarged area from the merged image. Nuclei were stained with DAPI (blue). (B) (E) Colocalization efficiency between core protein and early or late endosomes was analyzed by using Zeiss LSM Zen software. Error bars represent standard deviations of the mean result from 20 cells of two experiments. In parallel, the cell lysates were collected and then immunoblotted with antibodies against CD63 (C) and EEA1 (F). Results were quantified by PhosphorImager counting. The HCV-infected cells (at day 10 p.i.) were fixed either for immunofluorescence microscopy (G) or for thin-section electron microscopy (H and I). Cells were costained with anti-Rab5a (green) (G, left panel), -CD63 (green) (G, right panel) and -core protein (red). Lipid droplets (LDs) and nuclei were stained with BODYPI 493/503 (blue) and DAPI (white), respectively (G). Enlarged views of parts of every image are shown (insets). (H, left panel) Early endosome (EE) (white arrow) containing particles resembling HCV adjacent to the LDs. (I, left panel) MVB/late endosome (LE) containing particles resembling HCV and internal vesicles (white arrow). High-magnification images of the early endosome (H, right panel) and MVB/late endosome (I, right panel) harboring particles resembling HCV (black arrow).

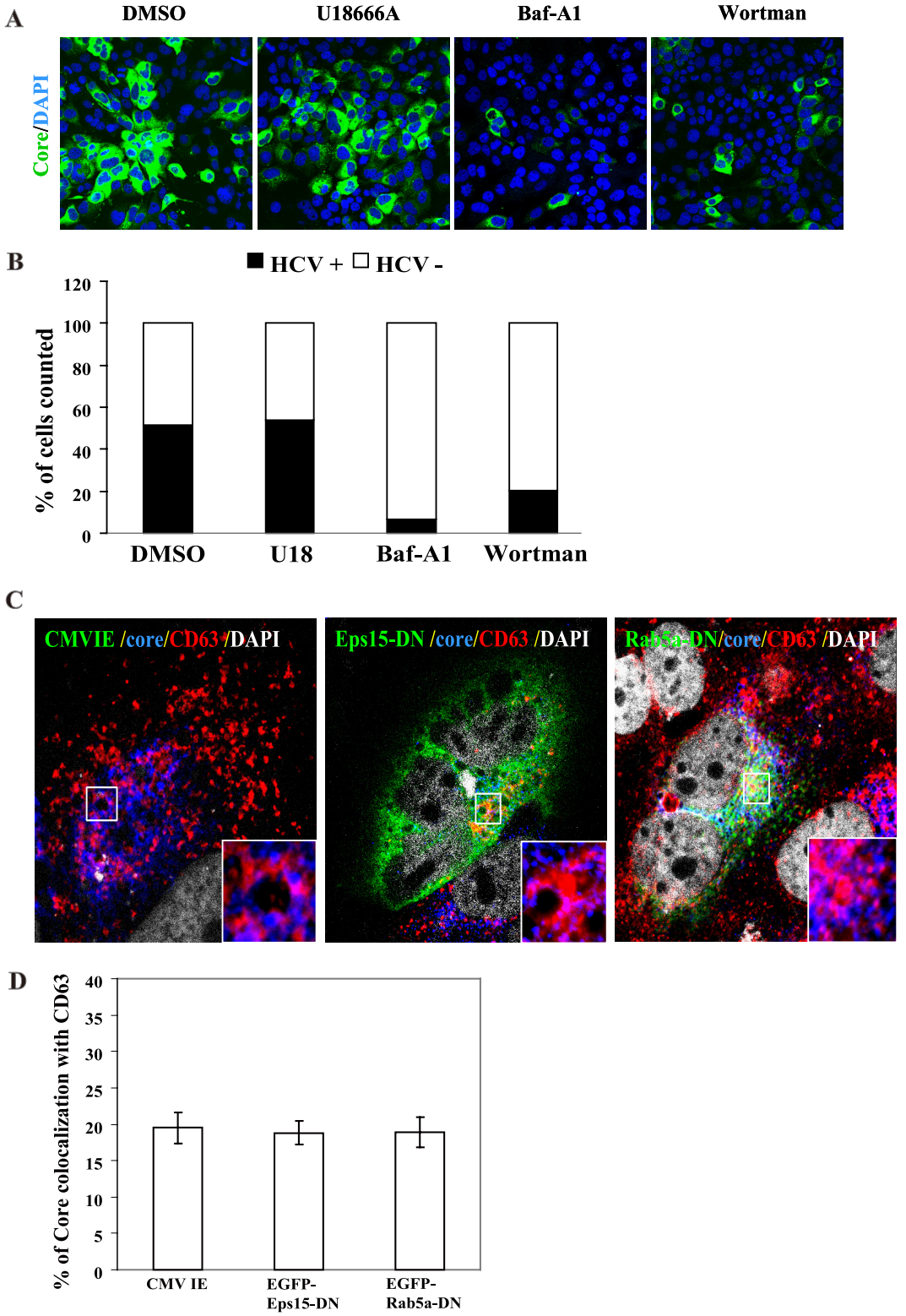

FIG. 4. HCV entry and RNA replication are not affected by inhibiting late endosome movement, and endosomal localization of core protein is not affected by inhibiting endocytosis. Huh7.5 cells were treated with the various drugs and 14 h later washed and inoculated with HCV Jc1. At 3 days p.i., cells were stained with anti-core protein antibody (green) and DAPI (blue) (A). The images were analyzed by using Metamorph and the proportion of cells (of 5,000 counted) expressing core protein was counted (B). (C) Colocalization of HCV core protein and late endosomes is not affected by DN mutants of Esp15 or Rab5a. HCV-infected cells (at day 5 p.i.) were transfected with a control plasmid pCMV-IE (C, left panel) or with dominant negative mutants of Eps15 (pEGFP-Eps15-DN) (C, middle panel) or Rab5a (pEGFP-Rab5a-DN) (C, right panel). At day 2 posttransfection, cells were labeled with antibodies specific for core protein (blue) and CD63 (red). Cells expressed EGFP-Eps15-DN or -Rab5-DN proteins (green). Nuclei were stained with DAPI (white). Enlarged views of parts of every image (insets) are shown. Colocalization of core protein and CD63 is depicted in magenta. (D) Results from colocalization analysis are shown using Zeiss LSM Zen software. Error bars represent standard deviations of the mean result from 20 cells of two experiments.

that colocalized with CD63 was 17% (Fig. 3B). After treatment with U18666A, a characteristic collapse of dispersed CD63 compartments to the perinuclear region of the cells was revealed (Fig. 3A, second row). Importantly, the colocalization of core protein with CD63 increased to 30% when the movement of late endosome was arrested by U18666A, whereas it was reduced to 2% and 7% by Baf-A1 and wortmannin treatments (Fig. 3A and B), respectively, suggesting that the movement of core protein was blocked by U18666A and accumulated in the juxtanuclear region. Additionally, EEA1-labeled distinct puncta, which are dispersed throughout the cytoplasm and partially colocalized with core protein in DMSO treatment (Fig. 3D, top row), were found clustered in the perinuclear region following treatments with U18666A and Baf-A1 (Fig. 3D, second and third rows). Correspondingly, the colocalization of core protein and EEA1 was increased after these treatments. In contrast, very little colocalization between core protein and EEA1 was seen after treatment with wortmannin (Fig. 3D, bottom row). The colocalization of core protein and EEA1 was 10% in the DMSO control, in contrast with 35% and 20% after treatments with U18666A and Baf-A1, respectively, and 4% after treatment with wortmannin (Fig. 3E). These data suggest that core protein was blocked by U18666A and accumulated in the juxtanuclear region. In parallel, the levels of CD63 and EEA1 protein in the lysates were determined by Western blotting. The results indicated that the total levels of CD63 and EEA1 were not altered by the various drug treatments (Fig. 3C and F, respectively). These results collectively indicate that the colocalization of core protein with CD63 or EEA1 and the release of virus particles depend on the motility of endosomes. Thus, we suggest that HCV core and/or the viral particles formed are transported from early to late endosomes.

The above results prompted us to characterize the location of the early and late endosomes in relation to the site of core-LD colocalization, where HCV assembly takes place (23). In HCV-infected cells (at day 10 p.i.), early endosomes (Fig. 3G, left panel) were colocalized with core protein and were located in juxtaposition to LDs, whereas the late endosomes were located far away from LDs (Fig. 3G, right panel). These data suggest that following the assembly of viral particles in juxtaposition to LDs, the HCV particles are transported through early to late endosomes. To gain further insight into the trafficking patterns of HCV particles in Huh7.5 cells, we performed electron microscopy of the HCV-infected cells (at day 10 p.i.). Particles resembling HCV were present in both the early endosomes adjacent to the LDs (Fig. 3H) and MVBs (late endosomes) (Fig. 3I). The morphology of these endosomal compartments is similar to that reported previously (34, 36). These results again suggest that the HCV particles formed are transported from early to late endosomes.

In order to rule out the possibility that the reduction in HCV particle secretion by endosome inhibitors (Fig. 2) was caused by the inhibition of endocytosis-mediated virus entry, we determined the percentage of cells that could be infected by HCV in the presence of endosome inhibitors. Cells were first treated with inhibitors of endosome movement, followed by HCV inoculation for 3 days. This analysis revealed that the same percentage of cells was infected and produced core protein following DMSO and U18666A treatments, 52% and 54%, respectively (Fig. 4A and B), demonstrating that U18666A did not affect HCV entry, and HCV could proceed normally to RNA replication. In contrast, Baf-A1 and wortmannin treatments yielded 7% and 20% (Fig. 4A and B), respectively, of infected cells, indicating that they blocked HCV entry, as previously reported (6, 21). Overall, these findings indicate that late endosome motility is dispensable for HCV entry and subsequent RNA replication and translation but is required for viral egress.

Moreover, we observed an almost complete block in virus infection after expression of either an Eps15 dominant negative (DN) mutant, EGFP-Eps15D95/295 (EGFP-Eps15-DN) (4), or a Rab5a dominant negative mutant, EGFP-Rab5a-S34N (EGFP-Rab5a-DN) (30), in naïve Huh7.5 cells (data not shown). This finding is consistent with a previous report (21). We further studied the effects of the DN mutants of Eps15 and Rab5a on the colocalization of core protein and the late endosomes to confirm that this colocalization was not due to the process of virus entry. Since the DN mutants of endocytosis will block HCV infection, we first performed virus infection followed by expression of the DN mutants. This strategy has been used to demonstrate that the trafficking of HIV-1 RNA and Gag protein to late endosome is independent of the endocytosed virus (19). EGFP-Eps15-DN and EGFP-Rab5-DN were transfected into HCV-infected cells (at day 5 p.i.). As shown in Fig. 4C, the localization of core protein with CD63 in these cells was not affected by the expression of these DN mutants; core protein remained well colocalized with CD63 in both the cell periphery and juxtanuclear positions in the multiple-cycle HCV growth assays. The calculated efficiency of colocalization of core protein with CD63 (19 to ~20%; Fig. 4D) was not altered. These results indicate that core protein localization with late endosomes is not the result of the accumulation of endocytosed viruses but rather represents the trafficking intermediates of the core protein during the late viral replication stages. Thus, we conclude that the late endosome-based secretory pathways are not involved in virus entry but rather deliver the assembled virions to the extracellular milieu.

Taken together, our results indicate that HCV egress requires the motility of early to late endosomes, which is microtubule dependent, and that this pathway is independent of the one required for virus entry. Thus, we postulate that following the assembly of virus particles in juxtaposition to LDs, the HCV particles are transported through early to late endosomes to the plasma membrane, where the membrane of late endosomes is fused with plasma membrane to release virions into the extracellular milieu. This transport appears to be important for HCV egress, but it is not clear how endosomes adapt in these processes. It is possible that HCV particles are transported into endosomes after their synthesis near LD. The endosome may facilitate transport of the virus particles to the plasma membrane or even to specialized cell surface domains, such as cell junctions. Notably, the tight junction protein claudin 1 has been reported to be required for HCV cell-to-cell transmission (33), which may help viruses to sequester away from the immune system.

We thank Takaji Wakita of the National Institute of Infectious Disease, Tokyo, Japan, for plasmid pJFH1, Alice Dautry-Varsat from the Pasteur Institute, France, for plasmids pEGFP-D3D2 Eps15 and pEGFP-Eps15D95/295 (a dominant negative mutant), Marino Zerial

from the Max Planck Institute of MCB and Genetics MPI-CBG Pfotenhauerstrasse, Germany, for plasmids pEGFP-Rab5a and pEGFP-Rab5a-S34N (a dominant negative mutant), Michinori Kohara from the Tokyo Metropolitan Institute of Medical Science, Japan, for rabbit polyclonal antibody against HCV core (RR8), and Charles M. Rice from the Center for the Study of Hepatitis C, Rockefeller University, New York, NY, for Huh7.5 cells.

REFERENCES

1. **Abid, K., V. Pazienza, A. de Gottardi, L. Rubbia-Brandt, B. Conne, P. Pugnale, C. Rossi, A. Mangia, and F. Negro.** 2005. An in vitro model of hepatitis C virus genotype 3a-associated triglycerides accumulation. J. Hepatol. **42:**744–751.
2. **Ai, L. S., Y. W. Lee, and S. S. Chen.** 2009. Characterization of hepatitis C virus core protein multimerization and membrane envelopment: revelation of a cascade of core-membrane interactions. J. Virol. **83:**9923–9939.
3. **Aniento, F., N. Emans, G. Griffiths, and J. Gruenberg.** 1993. Cytoplasmic dynein-dependent vesicular transport from early to late endosomes. J. Cell Biol. **123:**1373–1387.
4. **Benmerah, A., M. Bayrou, N. Cerf-Bensussan, and A. Dautry-Varsat.** 1999. Inhibition of clathrin-coated pit assembly by an Eps15 mutant. J. Cell Sci. **112**(Pt. 9)**:**1303–1311.
5. **Berger, K. L., J. D. Cooper, N. S. Heaton, R. Yoon, T. E. Oakland, T. X. Jordan, G. Mateu, A. Grakoui, and G. Randall.** 2009. Roles for endocytic trafficking and phosphatidylinositol 4-kinase III alpha in hepatitis C virus replication. Proc. Natl. Acad. Sci. U. S. A. **106:**7577–7582.
6. **Blanchard, E., S. Belouzard, L. Goueslain, T. Wakita, J. Dubuisson, C. Wychowski, and Y. Rouille.** 2006. Hepatitis C virus entry depends on clathrin-mediated endocytosis. J. Virol. **80:**6964–6972.
7. **Bomsel, M., R. Parton, S. A. Kuznetsov, T. A. Schroer, and J. Gruenberg.** 1990. Microtubule- and motor-dependent fusion in vitro between apical and basolateral endocytic vesicles from MDCK cells. Cell **62:**719–731.
8. **Booth, A. M., Y. Fang, J. K. Fallon, J. M. Yang, J. E. Hildreth, and S. J. Gould.** 2006. Exosomes and HIV Gag bud from endosome-like domains of the T cell plasma membrane. J. Cell Biol. **172:**923–935.
9. **Bost, A. G., D. Venable, L. Liu, and B. A. Heinz.** 2003. Cytoskeletal requirements for hepatitis C virus (HCV) RNA synthesis in the HCV replicon cell culture system. J. Virol. **77:**4401–4408.
10. **Boulant, S., M. W. Douglas, L. Moody, A. Budkowska, P. Targett-Adams, and J. McLauchlan.** 2008. Hepatitis C virus core protein induces lipid droplet redistribution in a microtubule- and dynein-dependent manner. Traffic **9:**1268–1282.
11. **Cai, Z., C. Zhang, K. S. Chang, J. Jiang, B. C. Ahn, T. Wakita, T. J. Liang, and G. Luo.** 2005. Robust production of infectious hepatitis C virus (HCV) from stably HCV cDNA-transfected human hepatoma cells. J. Virol. **79:** 13963–13973.
12. **Calistri, A., C. Salata, C. Parolin, and G. Palu.** 2009. Role of multivesicular bodies and their components in the egress of enveloped RNA viruses. Rev. Med. Virol. **19:**31–45.
13. **Corless, L., C. M. Crump, S. D. Griffin, and M. Harris.** 2010. Vps4 and the ESCRT-III complex are required for the release of infectious hepatitis C virus particles. J. Gen. Virol. **91:**362–372.
14. **Craven, R. C., R. N. Harty, J. Paragas, P. Palese, and J. W. Wills.** 1999. Late domain function identified in the vesicular stomatitis virus M protein by use of rhabdovirus-retrovirus chimeras. J. Virol. **73:**3359–3365.
15. **Gastaminza, P., S. B. Kapadia, and F. V. Chisari.** 2006. Differential biophysical properties of infectious intracellular and secreted hepatitis C virus particles. J. Virol. **80:**11074–11081.
16. **Goodman, J. M.** 2008. The gregarious lipid droplet. J. Biol. Chem. **283:** 28005–28009.
17. **Gousset, K., S. D. Ablan, L. V. Coren, A. Ono, F. Soheilian, K. Nagashima, D. E. Ott, and E. O. Freed.** 2008. Real-time visualization of HIV-1 GAG trafficking in infected macrophages. PLoS Pathog. **4:**e1000015.
18. **Kolesnikova, L., B. Berghofer, S. Bamberg, and S. Becker.** 2004. Multivesicular bodies as a platform for formation of the Marburg virus envelope. J. Virol. **78:**12277–12287.
19. **Lehmann, M., M. P. Milev, L. Abrahamyan, X. J. Yao, N. Pante, and A. J. Mouland.** 2009. Intracellular transport of human immunodeficiency virus type 1 genomic RNA and viral production are dependent on dynein motor function and late endosome positioning. J. Biol. Chem. **284:**14572–14585.
20. **Martin-Serrano, J., T. Zang, and P. D. Bieniasz.** 2001. HIV-1 and Ebola virus encode small peptide motifs that recruit Tsg101 to sites of particle assembly to facilitate egress. Nat. Med. **7:**1313–1319.
21. **Meertens, L., C. Bertaux, and T. Dragic.** 2006. Hepatitis C virus entry requires a critical postinternalization step and delivery to early endosomes via clathrin-coated vesicles. J. Virol. **80:**11571–11578.
22. **Mills, I. G., A. T. Jones, and M. J. Clague.** 1998. Involvement of the endosomal autoantigen EEA1 in homotypic fusion of early endosomes. Curr. Biol. **8:**881–884.
23. **Miyanari, Y., K. Atsuzawa, N. Usuda, K. Watashi, T. Hishiki, M. Zayas, R. Bartenschlager, T. Wakita, M. Hijikata, and K. Shimotohno.** 2007. The lipid droplet is an important organelle for hepatitis C virus production. Nat. Cell Biol. **9:**1089–1097.
24. **Nydegger, S., M. Foti, A. Derdowski, P. Spearman, and M. Thali.** 2003. HIV-1 egress is gated through late endosomal membranes. Traffic **4:**902–910.
25. **Pelchen-Matthews, A., B. Kramer, and M. Marsh.** 2003. Infectious HIV-1 assembles in late endosomes in primary macrophages. J. Cell Biol. **162:**443–455.
26. **Perez, M., R. C. Craven, and J. C. de la Torre.** 2003. The small RING finger protein Z drives arenavirus budding: implications for antiviral strategies. Proc. Natl. Acad. Sci. U. S. A. **100:**12978–12983.
27. **Perlman, M., and M. D. Resh.** 2006. Identification of an intracellular trafficking and assembly pathway for HIV-1 gag. Traffic **7:**731–745.
28. **Roohvand, F., P. Maillard, J. P. Lavergne, S. Boulant, M. Walic, U. Andreo, L. Goueslain, F. Helle, A. Mallet, J. McLauchlan, and A. Budkowska.** 2009. Initiation of hepatitis C virus infection requires the dynamic microtubule network: role of the viral nucleocapsid protein. J. Biol. Chem. **284:**13778–13791.
29. **Rouille, Y., F. Helle, D. Delgrange, P. Roingeard, C. Voisset, E. Blanchard, S. Belouzard, J. McKeating, A. H. Patel, G. Maertens, T. Wakita, C. Wychowski, and J. Dubuisson.** 2006. Subcellular localization of hepatitis C virus structural proteins in a cell culture system that efficiently replicates the virus. J. Virol. **80:**2832–2841.
30. **Stenmark, H., R. G. Parton, O. Steele-Mortimer, A. Lutcke, J. Gruenberg, and M. Zerial.** 1994. Inhibition of rab5 GTPase activity stimulates membrane fusion in endocytosis. EMBO J. **13:**1287–1296.
31. **Stone, M., S. Jia, W. D. Heo, T. Meyer, and K. V. Konan.** 2007. Participation of Rab5, an early endosome protein, in hepatitis C virus RNA replication machinery. J. Virol. **81:**4551–4563.
32. **Strecker, T., R. Eichler, J. Meulen, W. Weissenhorn, H. Dieter Klenk, W. Garten, and O. Lenz.** 2003. Lassa virus Z protein is a matrix protein and sufficient for the release of virus-like particles. J. Virol. **77:**10700–10705. (Erratum, **77:**12927.)
33. **Timpe, J. M., Z. Stamataki, A. Jennings, K. Hu, M. J. Farquhar, H. J. Harris, A. Schwarz, I. Desombere, G. L. Roels, P. Balfe, and J. A. McKeating.** 2008. Hepatitis C virus cell-cell transmission in hepatoma cells in the presence of neutralizing antibodies. Hepatology **47:**17–24.
34. **Tooze, J., and M. Hollinshead.** 1991. Tubular early endosomal networks in AtT20 and other cells. J. Cell Biol. **115:**635–653.
35. **Watanabe, T., E. M. Sorensen, A. Naito, M. Schott, S. Kim, and P. Ahlquist.** 2007. Involvement of host cellular multivesicular body functions in hepatitis B virus budding. Proc. Natl. Acad. Sci. U. S. A. **104:**10205–10210.
36. **Yi, J., and X. M. Tang.** 1999. The convergent point of the endocytic and autophagic pathways in Leydig cells. Cell Res. **9:**243–253.
37. **Zehmer, J. K., Y. Huang, G. Peng, J. Pu, R. G. Anderson, and P. Liu.** 2009. A role for lipid droplets in inter-membrane lipid traffic. Proteomics **9:**914–921.